

Behaviors and Characteristics Study of the Electron Beam for Lens System in a Scanning Electron Microscope

Mohammed A. Hussein

University of Kirkuk

College of agriculture / Hawija

Dept. of mechanization and agricultural equipment

mohdphy@yahoo.com

Mohanad Q. Kareem,

University of Kirkuk

College of Science

Dept. of physics

drmohanad33@gmail.com

Abstract

This work aims to study the behaviors and characteristics of the electron beam within the optical column in a thermionic scanning electron microscope (SEM) and the focusing capability using a numerical computation and an optics-based calculation. The beam spot size is estimated by theoretical calculation. Investigate the SEM performance for various design parameters through a numerical analysis and an optics-based calculation, a combination of two approaches gives more detailed information than a single approach in investigating an extremely small beam spot by demagnification through the magnetic lens system in a SEM column.

Keywords: Magnetic lens; Scanning electron microscopy; Thermionic emission; Numerical analysis; Beam trajectory.

1. Introduction

Represents a scanning electron microscope (SEM) is one the most

popular instruments used in measure nano/micro structures for this reason it is also well known as a material analysis equipment. In nanotechnology, a precise measurement less than the nanometer scale is necessary to measure a nano-size device. The SEM has a high resolution due to using electron gun emits electron beam with wavelength of less than 1 nm [1]. the electron gun is categorized into two types depending on the way of beam emission: ones a thermionic emission gun and others a field emission gun. In this article, we focus on a thermionic SEM and see how systematic design schemes of a lens system in a SEM column are provided. The highest resolution SEM has been developed using a field emission [2–4]. However, the field emission. SEM is extremely expensive and most components dealing with the electrons need to be placed in extremely higher vacuum state in the range of 10^{-10} Torr, while a thermionic SEM operates in around 10^{-7} Torr. A thermionic SEM still holds a high market

share due to its effectiveness over the cost. An actual resolution of SEM is 50 times larger than the theoretical limit because of irregular electron gun size, aberration, energy spread, etc. Therefore, new generation of SEMs is focused on improvement an electron beam source to give high brightness and low energy spread, and an electron lens system with less aberration.

To enhance the resolution of SEM Compared with the optical microscope, we use accelerated electrons of extremely short wavelength less than 0.01nm. While optical microscope use a visible light source in the range of 300–700nm wavelength, a SEM uses The electrons being accelerated by high voltage applied on the filament, , and being focused on the specimen surface by electro-magnetic lenses [5]. The SEM are similar to an optical microscope in the structure and principle. For focusing light rays in the optical microscope use us the Optical lenses instead of electromagnetic lenses in a SEM. Fundamental difference appear in a SEM. The electromagnetic lens consist of an electric coil pass through it the current, generates magnetic flux within a concentrated small volume by [6]. We can decrease the wavelength of an

electron beam by increasing the acceleration voltage applied on the emitted beam source, which is useful to the image resolution. There are many parameters constrains the enhancement of SEM resolution. Design a poor beam source as well as an improper lenses arrangement.

numerical analysis uses widely to facilitate the design of the electron lenses therefore munro used a finite element method from first order to analyze electron lenses.[7] By the Lorentz force The magnetic flux associated with acceleration voltage makes the electron beam travel along optical column and be focused at a focal point. The is by there are various factors effect on the focusing such as an electric current applied on the coil, geometry and arrangement of the lenses in the optical column, and acceleration voltage.

To increase the resolution of a SEM, the electron beam size and the energy spread must be decreased. A geometric optics should be clearly designed and manufactured. In addition, the following factors are particularly considered. once, the electron beam source size is to be controlled within a small spot size, and the final probe diameter after demagnification by the

subsequent lenses should be controlled within of nanometer. The other, chromatic aberration should be decreased, by placing a specially designed stigmator and the electron beams emitted from a filament must be sufficiently stabilized.

In this work, we focus on the design of the lens system by employing a numerical analysis and geometrical optics for the SEM. Through these analyses, beam focusing characteristics and the resulting lens aberrations can be estimated. The beam trajectory analysis under various selections of the lenses by simulating the SEM system using an Munro software [7], providing a guideline in designing an efficient SEM.

2. Numerical analysis of the electron optical system

The schematic diagram of

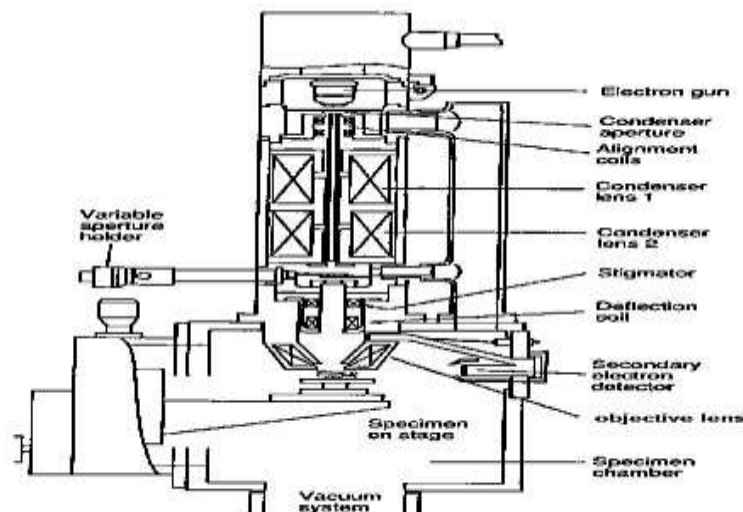


Figure. 1. Schematic structure of the thermionic SEM. [8]

thermionic SEM, as shown in Fig. 1 illustrate consist of an optical column, devices to improve the beam focusing characteristics, and a detector collecting secondary electrons emitted from the specimen. Electromagnetic lens to focus the electron beam spot. If the lens system is not appropriately designed or misaligned, the shape of a beam spot will be a bad shape or blurry. Therefore, a precise analysis of the beam focus is required to ensure a high-performance SEM in terms of small beam spot size and less aberration. we consider two methods: a numerical analysis using a beam tracing program M21 and a calculation based on a geometric optics. Therefore, a combination of the calculation and the numerical analysis gives a strong basis for an optimal design of the lens system in a SEM.

3. Background of the numerical analysis

Using M21 software from numerical analysis we performed An electron beam trajectory under the magnetic fields on three lenses. Firstly, analyze of distribution of the electromagnetic field for the designed lenses each magnetic flux is distributed around the lens and the magnitude is enough to deflect the electron beams. As the electron beams pass through three electromagnetic lenses, the final beam spot is formed after demagnification through the subsequent lenses, of which diameter is determined by the ratio of the focal lengths to the displacements among lenses.

Here, we introduce a principle of the electron beam tracing by using the governing equations. The equations describing the electromagnetic field generated by the magnetic enses are given by the Maxwell's equations as follows:

$$\nabla * E = - \frac{\partial B}{\partial t} \tag{1}$$

$$\nabla * H = J \tag{2}$$

$$\nabla . D = \rho \tag{3}$$

$$\nabla . B = 0 \tag{4}$$

Where E is the electric field intensity, B is the magnetic flux density, D is

the electric flux density, H is the magnetic field intensity, J is the current density, and r is the electrical resistivity. If we set the magnetic vector potential A given by Eq. (5), the distribution of A can be expressed as Eq. (6), by uniting Maxwell's equations:

$$B = \nabla * A \tag{5}$$

$$\frac{1}{\mu} \nabla * \nabla * A - \rho \frac{\partial A}{\partial t} = 0 \tag{6}$$

Where m is the permeability of the material. The distribution of A is then calculated by minimizing the vibrational functional [9]:

$$F = \int \omega \left[\frac{1}{\mu} (\nabla * A) \cdot (\nabla * A) - J \cdot A \right] d\omega = 0 \tag{7}$$

Based on the calculated magnetic fields, the electron beam tracing under the formed magnetic fields on each lens is performed by solving the paraxial ray Eq. (7):

$$r''(z) + \frac{e}{8mv} B^2(z) r(z) = 0 \tag{8}$$

where e/m is the charge/mass ratio of the electron and V is the beam voltage .

4. Magnetic lens system

In the electron beam tracing, the electromagnetic field for each

lens for given number of coil turns, electron current, and geometric properties is analyzed. The electromagnetic field distributions for the designed lenses are analyzed whether the magnetic flux is appropriately distributed around the lens and its magnitude is appropriate enough to deflect the electron beam. We numerically calculated the distribution of magnetic field of three lenses placed subsequently in the SEM column. Figure. 2 shows the analysis domain for the column containing three magnetic lenses: two condenser lenses (CL1 and CL2) and an objective lens (OL).

Table 1 summarizes the basic specifications of coils and corresponding current densities for three magnetic lenses. Here, we selected one case of current set for each lens. At this set, the SEM image was acquired and numerical and optics-based analyses were carried out. It is quite sure that different sets of coil current on each lens bring a different focal length and beam diameter. If the set of the lens currents possesses a reliable credibility by the analyses, the results by a different set of lens currents and acceleration voltage also have validity.

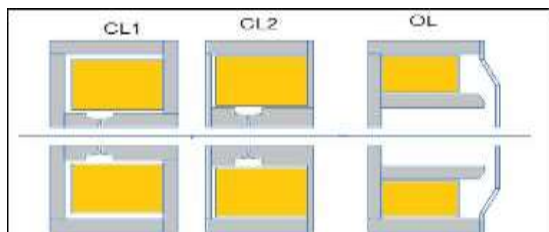


Figure. 2. Illustrate the SEM column.

Table 1. Basic specifications of coils for three magnetic lenses

Lens Kind	Excitation current (A)	No. of turns	Cross-sectional area (cm ²)	Current density (A/cm ²)
CL1	0.52	920	16.90	31.15
CL2	0.59	920	16.90	34.94
OL	1.90	600	10.45	112.09

Figure. 3 illustrates the distribution of magnetic flux in the column, showing that the magnetic fields are concentrated around the pole piece regions of the three magnetic lenses. Figure. 4 represent the variation of the axial component of magnetic flux (B_z) along the axial distance from the electron gun. It is found that the magnetic flux shows peak at the narrow-spaced pole-piece locations. Detailed results of three peak values are compared in Table 2. It is noted that the amount of the peak flux of the OL is smaller than those of two condenser lenses because the

OL has a larger gap of pole piece in order to install magnetic deflectors inside the lens. Even if coil currents on CL1 and CL2 are closely imposed, the corresponding magnetic fluxes on both lenses show a large difference. This implies that the magnetic flux on CL2 is affected by magnetic flux on CL1 because the length to the pole piece of CL2 from the end line of CL1 is shorter than that of CL1 from the start line of CL1. These analysis results are then connected to the ray tracing analysis to predict the beam trajectory.

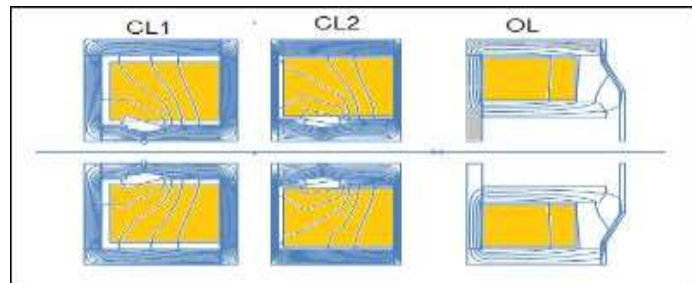


Figure 3. Distribution of the magnetic potential in the column.

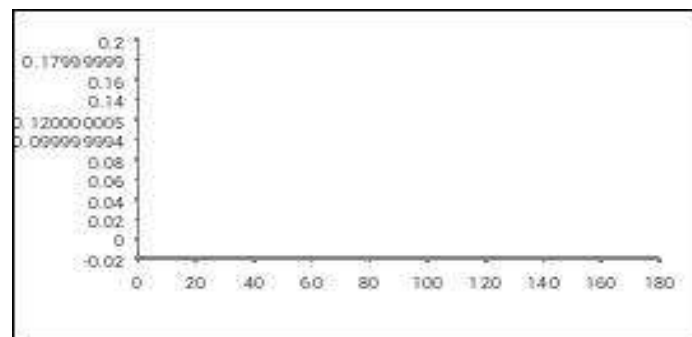


Figure 4. Variation of the axial component of magnetic flux.

Table 2. Summary of electromagnetic analysis of magnetic lenses

Lens Kind	Pole piece gap (mm)	Peak location (mm)	Peak flux (Tesla)
CL1	2.0	89	0.171
CL2	2.0	194	0.173
OL	8.0	390	0.108

5. Electron beam trajectory

A ray tracing of electron beams is then performed by taking into account the calculated magnetic field. Fig. 5 represents the estimated beam trajectory by solving the ray tracing equation, showing that three crossovers are formed by three magnetic lenses.

Table 3 summarizes the beam tracing results for the three lenses. The focal lengths are obtained by calculating the distances from the refracting position to the crossing position at each lens. Comparison of these results will be discussed in the next section.

Table 3 summarizes the beam tracing results for the three lenses

Lens Kind	Beam refraction position Z_p (mm)	Position of plane image Z_i (mm)	Focal length F (mm)
CL1	89.33	93.975	4.42
CL2	194.33	198.937	4.40
OL	361.92	372.950	10.34

As the electron beam is focused by the subsequent lenses arrangement and acceleration

voltage, it proceeds to the final specimen, hitting the specimen surface, and eventually generating

secondary electrons from the specimen. The secondary electrons are dedicated to the SEM image, which is determined by the amount of secondary electrons emitted from the surface of the specimen.

The amount of secondary electrons increases as the beam spot size is

small as possible to have strong current density. Thus, the beam spot size and uniform beam shape are crucial to obtain a high focused image. The beam spot size is approximately computed by employing a geometric optics which explains the demagnification process formed by lenses (Fig. 6).

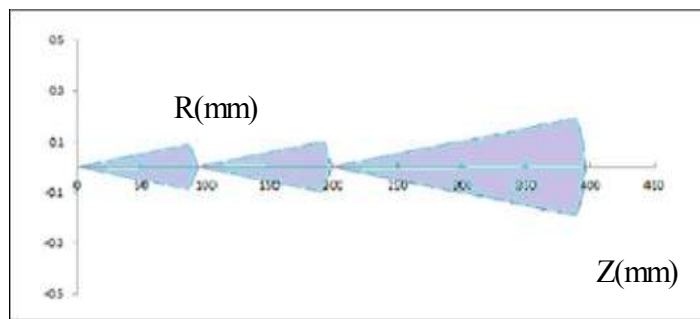


Figure. 5. Ray tracing results from the beam source to the image plane.

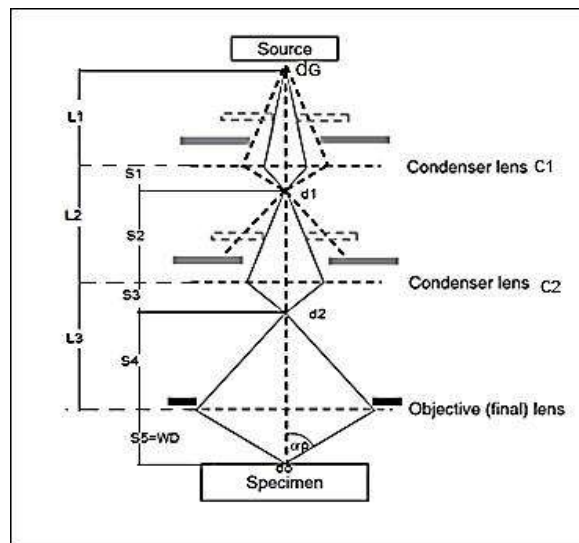


Figure. 6. Schematic diagram for focusing lenses.

The numerical analysis by commercial program, demonstrated in

the previous section, provides a detailed description of the beam tracing. However, it does not provide

all necessary information on beam characteristics. The beam intensity and the brightness are some of the characteristics not provided by numerical analysis. A calculation by geometric optics on the lens system supplements this weakness.

So far, we assumed that each magnetic flux $B_z(z)$ of the three lenses shows a symmetric shape, which makes the computation of the focal length simple as Eq. (11). However, even if the flux distributions of other two lenses keep almost symmetric bell shapes, the magnetic flux of the object lens is bell shaped but not symmetric: the left side of the shape is gentler than the right side. It limits the direct use of Eq. (10), hence a more precise calculation of magnetic flux is required. Here we adopt a numerical integration to obtain the focal lengths from the magnetic flux for three lenses, which is shown in eq. (10)

The results of focal lengths for each lens by numerical integration are shown in Table 4. We can see slightly different results compared with the results obtained by simple bell-shaped assumption on the magnetic flux. For a simple calculation, the focal length

computation based on the bell-shaped magnetic flux is still acceptable.

The axial magnetic flux is determined through a numerical analysis as introduced in the previous section. This implies that a different set of coil currents or pole piece shapes generates different magnetic flux, yielding a different focal length in the lens. Since the SEM consists of three lenses focusing the electron beam consecutively, the total demagnification of a three-lens system yields a final focused spot d_0 :

$$d_0 = \frac{f_1 f_2 f_3}{p_1 p_2 p_3} d_c \tag{9}$$

$$\frac{1}{f} = \frac{e}{8mV} \int_{-\infty}^{+\infty} B_z^2 dz \tag{10}$$

$$f = \frac{2a}{\pi k^2} \quad \text{for } k^2 \ll 1 \tag{11}$$

$$d_0 = \left(\frac{4I_p}{\pi^2 \beta} \right) \frac{1}{2\alpha_p^{-1}} \tag{12}$$

Where d_0 and d_c represent the final probe diameter and the beam diameter at the cathode, respectively. $f_{1,2,3}$ is the focal lengths for each lens and $p_{1,2,3}$ is the displacements between each lens center. Since it is not easy to measure d_c directly, a numerical analysis is carried out using munro software. The beam propagation from the cathode under bias voltage

of 50 V and the virtually focused beam diameter are estimated. According to the analysis, the beam diameter at the cathode after being focused by the biased voltage and acceleration voltage of 20 kV turns out to be around 33 mm.

Viewing Eq. (9), it is noted that once all focal lengths and displacements are determined the final probe diameter can be determined and the demagnification through three lenses is also computed.

Table 4. Comparison of the focal lengths

Lens Kind	Analytical solution (mm)	Analytical with numerical integral (mm)
CL1	5.11	7.65
CL2	6.45	7.62
OL	14.65	15.67

The probe diameter is estimated by employing Eq. (9) with the help of demagnification formed by the focal lengths computed from Eq. (10).

Table 5. Computation of focal lengths, aperture angles, and estimated probe diameter for given coil currents and acceleration voltage of 20 kV.

Lens Kind	CL1	CL2	OL
Current (A)	0.52	0.59	1.90
Maximum magnetic flux B_{max} (Tesla)	0.171	0.173	0.108
Half-width a (mm)	4.0	3.5	9
Focal length f_1, f_2, f_3 (mm)	4.42	4.40	10.34
Lens length to center p_1, p_2, p_3 (mm)	90	105	170
Aperture angle α_p (rad.)	0.035 Diameter of 1000 μ m	0.060 Diameter of 1000 μ m	0.008 Diameter of 200 μ m

6. Conclusions

The analysis of an electron

beam tracing and focusing in a lens system contributes to an optimal design of the lens system in an SEM before manufacture. This analysis necessary To secure a highly demagnified beam spot. the focal lengths formed by the magnetic flux on magnetic lenses, which are generated by the coil current and the shape of pole piece, were investigated. To obtain a minimized probe beam spot, the demagnification ratio on each lens should be as large as possible unless the lenses have undesirable aberrations. Employed both numerical analysis program and optics calculation to analyze the focal length. Two ways were reciprocal in terms of being able to extract complementary parameters and they showed a quite satisfactory agreement. When two ways are integrated, rather than a single way, in the early stage of lens system design can be easily obtained for the desired focal length and other parameters. From the a numerical analysis and geometric optics, The probe diameter, which is an important factor in SEM performance, can be estimated. The

validity of the numerical analysis and optics-based computation for the lens system is proved by measuring the probe diameter that results in the estimation of the probe diameter.

References

- [1].J.I. Goldstein, D.E. Newbury, P. Echlin, D.C. Joy, C. Fiori, E. Lifshin, (1981)," Scanning Electron Microscopy and X-Ray Microanalysis", Plenum .Press, New Yor .
- [2].A. Khursheed, (2000)," Magnetic axial field measurements on a high resolution miniature scanning electron microscope", Rev. Sci. Instrum. 71 (4).Pp 1712–1715.
- [3].T.H.P. Chang, M.G.R. Thomson, M.L. Yu, E. Kratschmer, H.S. Kim, K.Y.Lee, S.A.Rishton, S. Zolgharnain, (1996)," Electron beam technology-SEM to micro column", Micro- electron. Eng. 32.Pp113–130.
- [4].H.W. Mook, P. Kruit, (1999)," Optics and design of the fringe field mono chromator for a Schottky field emission gun", Nucl. Instrum. Methods Phys.

Res. A 427. Pp 109–120.

- [5]. P.W. Hawkes, (1982), Magnetic Electron Lenses, Springer, Berlin, Heidelberg, New York,
- [6]. A.S.A. Alamir, (2003), A study on effect of current density on magnetic lenses, Optik 114 (2). Pp 85–88.
- [7]. E. Munro, (1975), "A set of computer programs for calculating the properties of electron lenses", Cambridge University, Eng., Dept., Report CUED/B-ELECT/TR 45..
- [8]. J.J. Bozzola and L.D. Russell, (1999), "Electron Microscopy", 2nd Edition Copyright by Jones and Bartlett Publishers, Inc.
- [9]. Jon Orloff, (2004), Handbook of Charged Particle Optics, CRC Press, New York,.